Cell

The *lta4h* Locus Modulates Susceptibility to Mycobacterial Infection in Zebrafish and Humans

David M. Tobin,[1] Jay C. Vary, Jr.,[2,10] John P. Ray,[1,10] Gregory S. Walsh,[5] Sarah J. Dunstan,[6,7] Nguyen D. Bang,[8] Deanna A. Hagge,[9] Saraswoti Khadge,[9] Mary-Claire King,[2,3] Thomas R. Hawn,[2] Cecilia B. Moens,[5] and Lalita Ramakrishnan[1,2,4,*]

[1]Department of Microbiology
[2]Department of Medicine
[3]Department of Genome Sciences
[4]Department of Immunology
University of Washington, Box 357242, Seattle, WA 98195, USA
[5]Howard Hughes Medical Institute and Division of Basic Science, Fred Hutchinson Cancer Research Center, Seattle, WA 98109, USA
[6]Oxford University Clinical Research Unit, Hospital for Tropical Diseases, 190 Ben Ham Tu, Quan 5, Ho Chi Minh City, Vietnam
[7]Centre for Tropical Medicine, Nuffield Department of Clinical Medicine, Oxford University, Oxford OX3 7LJ, UK
[8]Pham Ngoc Thach Hospital for Tuberculosis and Lung Disease, Ho Chi Minh City, Vietnam
[9]Mycobacterial Research Laboratory, Anandaban Hospital, Kathmandu, Nepal
[10]These authors contributed equally to this work
*Correspondence: lalitar@uw.edu
DOI 10.1016/j.cell.2010.02.013

SUMMARY

Exposure to *Mycobacterium tuberculosis* produces varied early outcomes, ranging from resistance to infection to progressive disease. Here we report results from a forward genetic screen in zebrafish larvae that identify multiple mutant classes with distinct patterns of innate susceptibility to *Mycobacterium marinum*. A hypersusceptible mutant maps to the *lta4h* locus encoding *leukotriene A_4 hydrolase*, which catalyzes the final step in the synthesis of leukotriene B_4 (LTB_4), a potent chemoattractant and proinflammatory eicosanoid. *lta4h* mutations confer hypersusceptibility independent of LTB_4 reduction, by redirecting eicosanoid substrates to anti-inflammatory lipoxins. The resultant anti-inflammatory state permits increased mycobacterial proliferation by limiting production of tumor necrosis factor. In humans, we find that protection from both tuberculosis and multibacillary leprosy is associated with heterozygosity for *LTA4H* polymorphisms that have previously been correlated with differential LTB_4 production. Our results suggest conserved roles for balanced eicosanoid production in vertebrate resistance to mycobacterial infection.

INTRODUCTION

M. tuberculosis (*Mtb*) infection triggers a stereotypic series of host responses. Phagocytes are recruited rapidly to the infection site where they engulf mycobacteria and transport them to deeper tissues (Wolf et al., 2007). Pathogenic mycobacteria can resist early host defenses, allowing them to establish residence in phagocytes (Russell, 2007). Once in tissues, infected macrophages recruit additional macrophages and other immune cells to form granulomas, complex host immune structures within which mycobacteria can persist indefinitely, even in the face of a focused host immune response (Russell, 2007). The interplay between mycobacterium and host draws on multiple pathways, each of which could potentially be modulated to influence outcome. For instance, mycobacteria could be eradicated by the innate immune defenses of phagocytes or counter these defenses to grow within. The forming granuloma could promote bacterial expansion and dissemination resulting in acute disease but may eventually curtail or even eradicate infection as adaptive immunity is invoked (Davis and Ramakrishnan, 2009).

Wide variation in tuberculosis (TB) susceptibility, progression and severity resulting from apparently similar infectious exposures is well-recognized (Cobat et al., 2009). Host factors appear to be major contributors to variation in TB outcomes. Human genetic studies of patients susceptible to infection by normally avirulent mycobacteria have confirmed the importance of the IL-12/IFN-γ circuit in human resistance to mycobacterial infections (Fortin et al., 2007). Analysis of inbred mouse strains and, more recently, of human polymorphisms has suggested that innate immune determinants also play a role in protection from mycobacterial infection in solo and in concert with adaptive immunity (Fortin et al., 2007; Pan et al., 2005). Similarly, host genetics play a critical role in infection outcomes with the related pathogen *Mycobacterium leprae,* the causative agent of leprosy (Alter et al., 2008). These outcomes range from a typically mild paucibacillary (tuberculoid) form to a severe disfiguring multibacillary (lepromatous) form (Scollard et al., 2006).

Zebrafish larvae infected with their natural pathogen *M. marinum* (*Mm*), a close genetic relative of *Mtb*, have proved useful in understanding mycobacterial pathogenesis and immunity (Tobin and Ramakrishnan, 2008). Zebrafish, like mammals, are dependent on adaptive immunity for maximal control of TB (Swaim et al., 2006). However, only innate immunity is operant in the larval stages, allowing assessment of the contribution of innate immunity to resistance and pathogenesis (Davis et al., 2002). The larvae are optically transparent, allowing visualization of the early steps of mycobacterial infection in whole live animals (Davis et al., 2002). This real-time monitoring combined with reverse genetic analysis of known host determinants (e.g., tumor necrosis factor) has led to an expanded understanding of the innate immune response to mycobacterial infection (Clay et al., 2008; Volkman et al., 2010). Here, we have exploited the genetic tractability of the zebrafish to conduct a forward genetic screen, directly identifying, in vivo, host determinants of resistance to infection. We have used a positional cloning approach to identify *lta4h* as a susceptibility locus. Then by combining real-time imaging with genetic and small molecule interception of relevant pathways, we have revealed a role for LTA4H in regulating the balance between pro- and anti-inflammatory eicosanoid derivatives of arachidonic acid (Serhan, 2007). Finally, we have extended our findings to uncover associations between human *LTA4H* polymorphisms influencing levels of LTB_4 production and susceptibility to two human mycobacterial diseases: TB in a Vietnamese population and leprosy in a Nepali population.

A Genetic Screen Yields Three Mutant Classes

We performed a gynogenetic diploid screen on zebrafish larvae (Beattie et al., 1999) (Figures 1A and 1B). Briefly, eggs were squeezed from F_1 mothers heterozygous for N-ethyl-N-nitrosourea (ENU)-mutagenized chromosomes. Haploid embryos were subjected to early pressure to generate fully diploid embryos whose only genetic contribution was maternal. Clutches of 20–50 larvae each from 355 independent F_1 females were infected with 150-250 green fluorescent *Mm* and assessed by fluorescence microscopy at 4 days post-infection (dpi). By 4 dpi, wild-type (WT) infection is consistently characterized by the presence of individual infected macrophages as well as discrete early granulomas (organized aggregates of differentiated macrophages) (Davis et al., 2002) (Figures 1C, 1E, and 1G).

Three mutant classes emerged from our screen (Figures 1D, 1F, and 1H). The first class had abundant infected macrophages, despite which they formed no or limited granulomas even when challenged with high infection doses for longer periods (Figures 1C, 1D, 1I, and 1J). This host mutant phenotype is reminiscent of infections with the attenuated bacterial mutant lacking the RD1/ESX-1 secretion system, or zebrafish deficient in matrix metalloproteinase 9 (MMP9) in which granulomas do not form despite abundant bacterial growth within individual macrophages (Volkman et al., 2010). Preliminary observations suggested that these mutants have attenuated infection, similar to the bacterial RD1/*esx-1* and host MMP9 deficiencies. The second mutant class displayed resistance to infection that was apparent at an earlier step of pathogenesis, with reduced bacterial burdens in individual macrophages even prior to granuloma formation (Figure 1F). This phenotype could be due to enhanced macrophage microbicidal capacity, perhaps resulting from mutations in innate immunoregulatory pathways (Liew et al., 2005).

The third and most common mutant class was hypersusceptible to *Mm* infection, displaying increased bacterial growth relative to WT siblings (Figures 1G and 1H), a phenotype similar to that seen when macrophages are absent or when TNF signaling is abrogated (Clay et al., 2007, 2008). Thus, this screen identified multiple mutant classes with mycobacterial susceptibility phenotypes predicted by observational studies in the zebrafish and by human epidemiological studies suggesting that some individuals may clear TB even before the onset of adaptive immunity (Cobat et al., 2009).

Mutant Mapping via a Bacterial Cording Phenotype

As first described by Koch in 1882 (Koch, 1882), virulent *Mtb* in culture takes on a distinctive corded appearance characterized by intertwined serpentine rope-like structures (Middlebrook et al., 1947). Long an in vitro correlate of virulence, cording was recently recognized to occur in vivo under circumstances in which *Mm* grows extracellularly rather than within macrophages (Clay et al., 2008). In the hypersusceptible mutant *fh112*, we found that the areas of increased bacterial growth (Figure 1H) displayed bacterial cording (Figure 2A) which was seldom detected in WT siblings, and which followed the expected Mendelian frequencies in crosses between *fh112*/+ heterozygotes (Figure 2B). We could therefore use bacterial cording as a sensitive and specific reporter to map *fh112* after crossing to the polymorphic WT WIK strain. Mutants were selected from infected progeny of heterozygous carrier crosses based on the presence of cording at 4 dpi. We mapped *fh112* to a region of zebrafish chromosome 4, between the marker z10062 and a SNP in a zebrafish ortholog of the PRKWNK1 gene (Figure 2C). The physical region defined by this interval contains several genes, including the zebrafish ortholog of the leukotriene A_4 hydrolase (*lta4h*) gene, known to be involved in proinflammatory eicosanoid synthesis in mammals (Figure S1) (Haeggstrom, 2004) and we pursued this gene as a leading candidate.

Analysis of *lta4h* expression in WT and *fh112* mutant fish showed that while *lta4h* mRNA was not induced by infection in WT fish, *lta4h* mRNA was decreased approximately 10-fold in infected mutants as compared to WT siblings (Figure 2D). However, when we sequenced the coding region and exon/intron boundaries of all 19 exons of *lta4h* in *fh112* mutants (Figure S1B) we found no mutations, suggesting that *fh112* might be a mutation in a regulatory region. To rule out the alternative possibility that the mutation lay in a neighboring locus and had indirect effects on *lta4h* expression, we searched for a second, molecularly identifiable *lta4h* allele. We identified a zebrafish line with a 7 kb retroviral insertion in the seventh exon of *lta4h* from a commercially available library of frozen sperm (Figure 2E and Figure S1B). The retroviral insertion *zm5961* decreased *lta4h* mRNA levels in both infected and uninfected larvae (Figure 2D). Analysis of mRNA remnants in the *zm5961* mutant identified an mRNA species that includes an in-frame deletion, corresponding to 88 amino acids (Figure S1B). Progeny from a *zm5961*/+ incross showed the expected increased frequency of cording (Figures S1C and S1D). We confirmed that *fh112* is an allele of

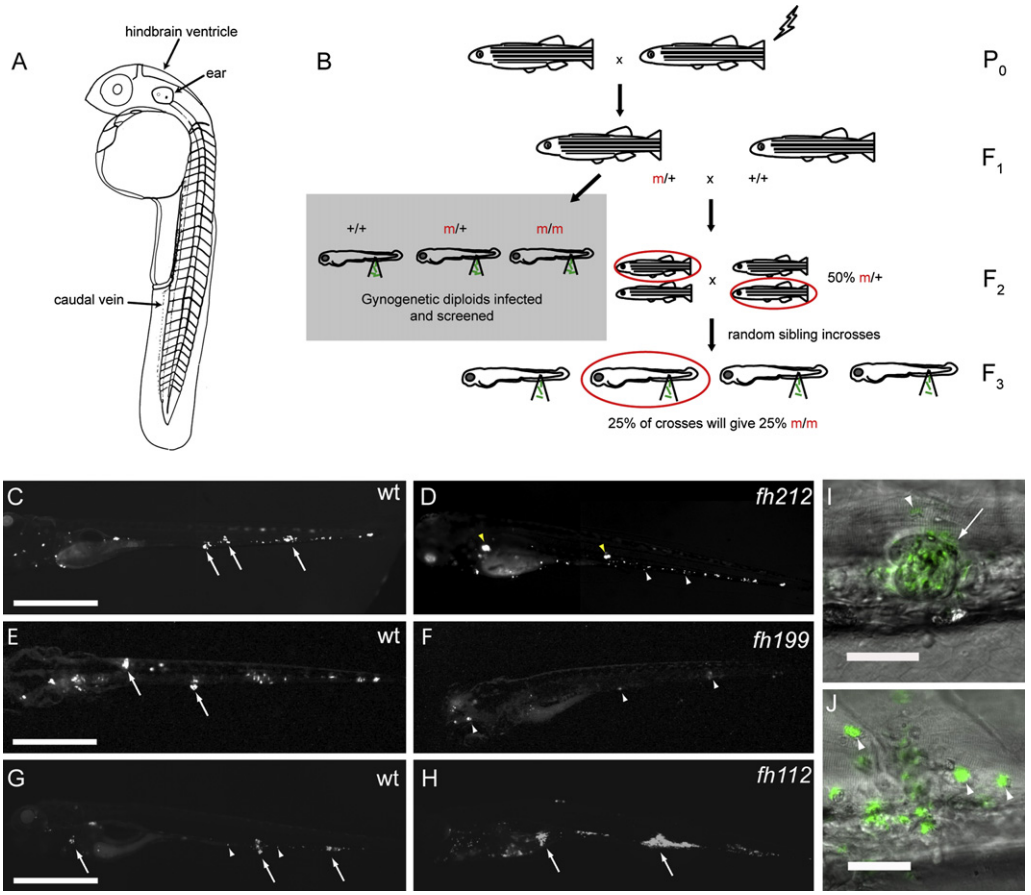

Figure 1. A Forward Genetic Screen Identifies Zebrafish Mutants with Altered Susceptibility to Mm Infection

(A) Diagram of zebrafish larva anatomy showing injection sites used in this study.

(B) Schematic diagram of forward genetic screen showing derivation of F_2 gynogenetic diploid embryos infected at two dpf. Potential mutants were confirmed by backcrossing the corresponding F_1 female and recovering the observed mutation in the F_3 generation.

(C–H) Fluorescence images of WT and mutant sibling fish at 5 dpi with equivalent bacterial inocula. Arrows, granulomas; white arrowheads, individual infected macrophages; yellow arrowheads, pairs of highly infected macrophages out of the focus plane that have not formed granulomas. Scale bars, 500 μm.

(C) WT and (D) aggregation mutant *fh212* sibling.

(E) WT and (F) resistant mutant *fh199* sibling.

(G) WT and (H) hypersusceptible mutant *fh112* sibling.

(I and J) Fluorescence and Differential Interference Contrast (DIC) overlay of 6 dpi WT fish with granuloma (arrow) (I) and aggregation mutant *fh141* sibling (J) with highly infected macrophages (arrowheads) that have not aggregated. The scale bar represents 50 μm.

lta4h by performing complementation analysis with the *fh112* and *zm5961* mutants. Heterozygous crosses of *fh112*/+ animals with *zm5961*/+ animals resulted in substantial cording at 5 dpi (Figure 2B). Control crosses of animals heterozygous for either allele with WT animals showed no cording, even with inocula as high as 350 CFU (data not shown; n = 21 for *fh112*/+ and n = 17 for *zm5961*/+, respectively).

We next characterized *lta4h* expression pattern in both WT and mutant larvae. In mammals, *lta4h* is expressed in myeloid cells (Peters-Golden and Henderson, 2007). Fluorescent in situ hybridization analysis in 2 days post-fertilization (dpf) uninfected zebrafish revealed expression in a phagocyte population of the caudal hematopoietic tissue that corresponds to both macrophages and neutrophils (Murayama et al., 2006) (Figure 2F). We confirmed that there was no reduction in macrophage and neutrophil numbers in uninfected three dpf *zm5961* homozygotes by neutral red staining and Sudan black staining, respectively (Figures S2A–S2D) (Herbomel et al., 2001; Le Guyader et al., 2008). However, *lta4h* expression was weakly or not detectable in phagocytes of *zm5961* homozygotes compared to their WT or heterozygous siblings (data not shown). Moreover, *zm5961*/*fh112* heterozygotes had reduced expression compared to siblings with one WT *lta4h* allele, confirming the non-complementation results observed for the infection phenotype (Figure 2G).

We characterized further the effect of *lta4h* on susceptibility by using morpholino oligonucleotides (MO) (Nasevicius and Ekker, 2000) to inhibit its translation. Injection of the *lta4h* MO resulted in phenocopy of the *fh112* mutant hypersusceptibility (Figure 3A and Figure 1H). Compared to controls, bacterial burden in *lta4h* morphants was increased 1.7 ± 0.3 (SEM) fold very early after infection, prior to granuloma formation and 7.6 ± 2.0 (SEM) fold

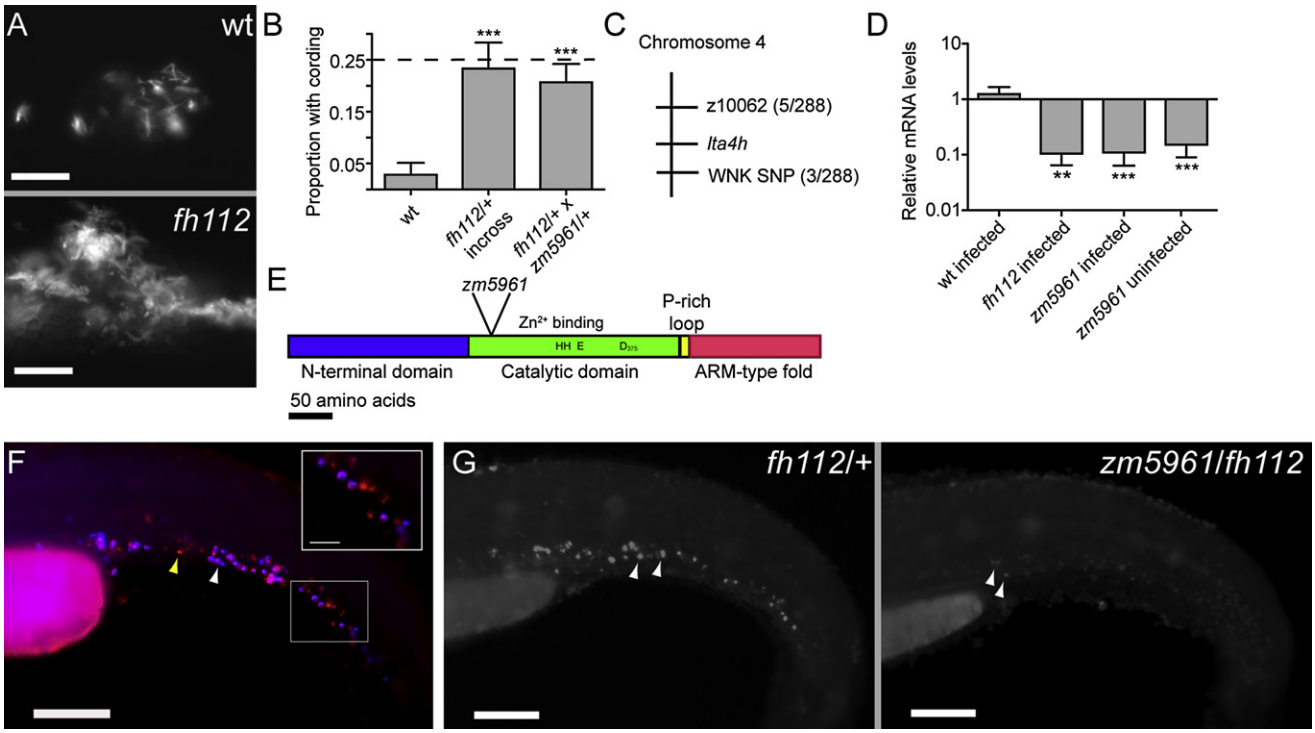

Figure 2. Mutations in the *leukotriene A_4 hydrolase* Gene Result in Decreased *lta4h* mRNA Expression and Increased Susceptibility to Mycobacterial Infection

(A) Fluorescence images of infection foci at 5 dpi with initial dose of 115 bacteria showing well-formed granuloma in WT fish (top) and profuse bacterial clusters showing cording morphology in hypersusceptible mutant *fh112* sibling (bottom). The scale bar represents 25 μm.

(B) Proportion of fish with cording morphology at 5 dpi with 150–250 bacteria in five independent clutches of 50–100 animals each of *fh112*/+ heterozygote or WT crosses and three independent clutches of 20–25 animals each from *fh112*/+ x *zm5961*/+ heterozygote crosses. Dotted line represents the theoretical maximum for a completely penetrant recessive mutation. Error bars represent the standard deviation (SD). ***$p < 0.001$ (one-way ANOVA with Tukey's post-test).

(C) Genetic map of *fh112* placing it between the polymorphic markers z10062 and a SNP in a PRKWNK1-related gene on zebrafish chromosome 4. Parentheses indicate the number of recombination events as a ratio of the total number of informative meioses scored.

(D) Mean *lta4h* RNA levels measured by qRT-PCR from 3–5 biological replicates of 30 fish. Infected *fh112* mRNA assessed at 4 dpi, infected and uninfected *zm5961* RNA at three dpf (1 dpi for infected *zm5961* fish). Fold difference expressed relative to matched WT uninfected controls. **$p < 0.01$; ***$p < 0.001$ (ANOVA with Tukey's post-test). Error bars represent the SD.

(E) Gene structure of zebrafish *lta4h* with location of the *zm5961* insertion and key conserved residues in the catalytic domain indicated (Haeggstrom, 2004).

(F) Fluorescent in situ hybridization (FISH) of *lta4h* (red) combined with *mpo* antibody staining for neutrophils (blue) in caudal hematopoietic tissue of two dpf uninfected fish. Yellow arrowhead, *lta4h*-staining, *mpo*-negative presumed macrophage. White arrowhead, dual staining neutrophil. Scale bar, 100 μm. Inset scale bar represents 25 μm.

(G) *lta4h* FISH in uninfected *fh112*/+ heterozygote (left) and *zm5961/fh112* non-complementing sibling (right) at two dpf. Arrowheads point to brightly staining cells in *fh112*/+ heterozygote and to weakly-expressing cells in non-complementer. The scale bar represents 100 μm.

See also Figure S1.

at 6 dpi (Figure 3B). This increased bacterial burden corresponded to increased mortality among infected morphants and increased bacterial cording (Figures 3C–3E). In summary, we mapped *fh112* susceptibility to the *lta4h* locus and show that reduced phagocyte expression of *lta4h* correlates with early susceptibility, increased extracellular bacterial growth and cording. Finally, similar to genetic *lta4h* deficiency, treatment of WT fish with 100 μM of the LTA4H inhibitor bestatin resulted in increased bacterial growth with cording (Figures 3F–3H) (Orning et al., 1991).

lta4h Interacts with the TNF Signaling Pathway

Previously, we had observed bacterial cording in two host gene knockdowns that altered pathogenesis at discrete steps: in macrophage-deficient (PU.1) morphants, and in TNF signaling deficiency produced by the TNF-receptor 1 (TR1) MO (Clay et al., 2007; Clay et al., 2008). The known functions of LTB_4 as a macrophage chemoattractant and a proinflammatory molecule suggested that *lta4h* cording could be related to either the PU.1 or TR1 morphant mechanisms. We asked whether *lta4h* deficiency reduces macrophage chemoattraction to infecting bacteria, thereby promoting extracellular bacterial growth and cording. We confirmed that LTB_4 functions as a macrophage chemoattractant in the zebrafish: its injection into the hindbrain ventricle (HBV) of WT larvae (Figure 1A) induced rapid recruitment of macrophages (Figure 4A; Movie S1). However, *lta4h* deficiency induced by MO treatment of either WT or mutant larvae compromised neither mycobacterially-induced recruitment to the

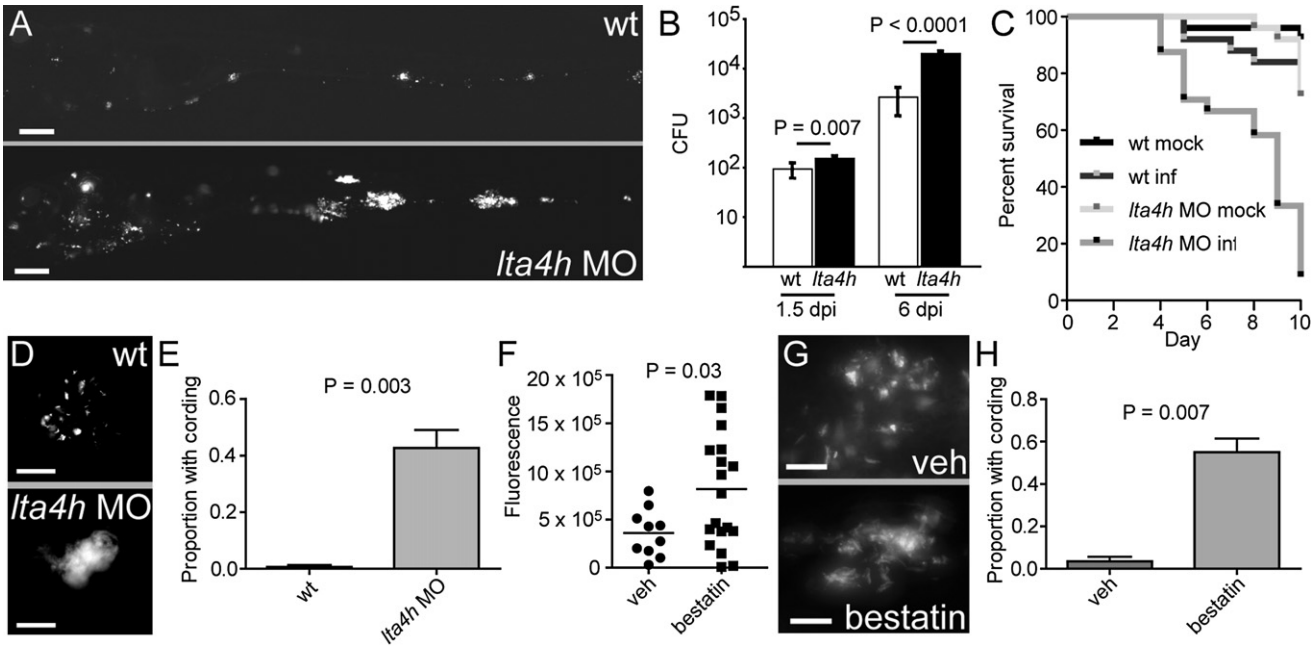

Figure 3. *lta4h* MO Knockdown Results in Increased Susceptibility to Mm

(A) Representative fluorescence images of control (top) and *lta4h* morphant (bottom) fish 5 dpi with 173 bacteria. The scale bar represents 200 μm.

(B) Mean bacterial loads per embryo for control (wt) and *lta4h* morphant embryos at 1.5 and 6 dpi with 150 bacteria (n = 4 groups of 5 animals for each time point). Error bars represent the SD.

(C) Survival of control and *lta4h* morphant fish mock-injected or injected with 177 bacteria (n = 25 per group). Hazard Ratio for death of infected morphants = 9.0, $p < 0.0001$ (Kaplan Meier method with log-rank [Mantel-Cox] test). Data representative of three independent experiments.

(D) Fluorescence image of non-cording bacteria within a granuloma in control animals (top) and cording bacteria in *lta4h* morphant (bottom) at 5 dpi with infection dose of 150 bacteria. The scale bar represents 20 μm.

(E) Mean proportion of animals with cording in three independent groups of 15–40 animals 4 dpi with 173 bacteria. $p = 0.003$ (Student's unpaired t test). Error bars represent the standard error of the mean (SEM).

(F) Bacterial burden at 5 dpi as determined by fluorescence pixel counts (FPC) for vehicle-treated or 100 μM bestatin-treated animals after injection with ~150 CFU Mm. $p = 0.03$ (Student's unpaired t test).

(G) Fluorescence image of non-cording bacteria within a granuloma in control animals (top) and cording bacteria in animals treated with 100 μM bestatin (bottom) at 5 dpi as described in (F). The scale bar represents 10 μm.

(H) Quantitation of cording at 4 dpi in five independent groups of 10–30 animals treated with vehicle or 100 μM bestatin after injection with 100–200 CFU Mm. $p = 0.007$ (Student's unpaired t test). Error bars represent the SEM.

HBV nor bacterial phagocytosis (Figures 4B, S2E, and S2F). Thus macrophage recruitment or phagocytosis defects were unlikely to be the cause of hypersusceptibility of *lta4h* deficient animals.

We next assessed if the *lta4h* mutation impacts the TNF pathway, critically important for resistance to mycobacteria in humans, mice and zebrafish (Clay et al., 2008; Flynn et al., 1995; Keane et al., 2001). We confirmed that LTB_4 induces TNF expression in WT zebrafish as in mammals (Goldman et al., 1993). Injection of $\sim 1.5 \times 10^{-14}$ mol LTB_4 into the caudal vein of uninfected larvae induced *tnf* mRNA expression in WT embryos 3.6 ± 0.7 (SEM)-fold over mock at 2.5 hr. In infected larvae, *lta4h* mRNA and *tnf* mRNA were both expressed early in granuloma macrophages (Figure 4C). However *lta4h* deficient fish had reduced induction of TNF upon infection. When we separated infected *fh112* mutants and their WT siblings from a heterozygous incross based on cording at 4 dpi, we found 3.7 ± 1.3 (SEM) fold less *tnf* mRNA in the mutants. To assess whether *tnf* reduction occurred early in infection, we used the molecularly-identifiable *zm5961* allele; infected *zm5961* animals expressed 7.3-fold less *tnf* mRNA than WT at 1 dpi (Figure 4D).

Next we detailed the infection phenotypes of *lta4h*-deficient larvae to determine if they shared specific attributes of TNF signaling-deficient animals. We previously identified the primary consequence of TNF deficiency to be increased bacterial growth within macrophages leading to increased granuloma formation followed by necrotic death of the infected macrophages (Clay et al., 2008). The Mm *erp* mutant is attenuated for intracellular growth within individual macrophages, and its attenuation and macrophage growth defect are rescued by TNF signaling blockade (Clay et al., 2008). Similarly, infected *lta4h* morphant embryos allowed increased overall growth of the *erp* mutant (Figures 4E and 4F), also showing increased bacterial growth in individual macrophages even prior to granuloma formation (Figure 4G). Second, *lta4h* deficiency induced accelerated kinetics of granuloma formation similar to TNF deficiency (Figures 4H–4J) (Clay et al., 2008). Finally, granulomas in *lta4h*-deficient animals became acellular as evidenced by loss of neutral red

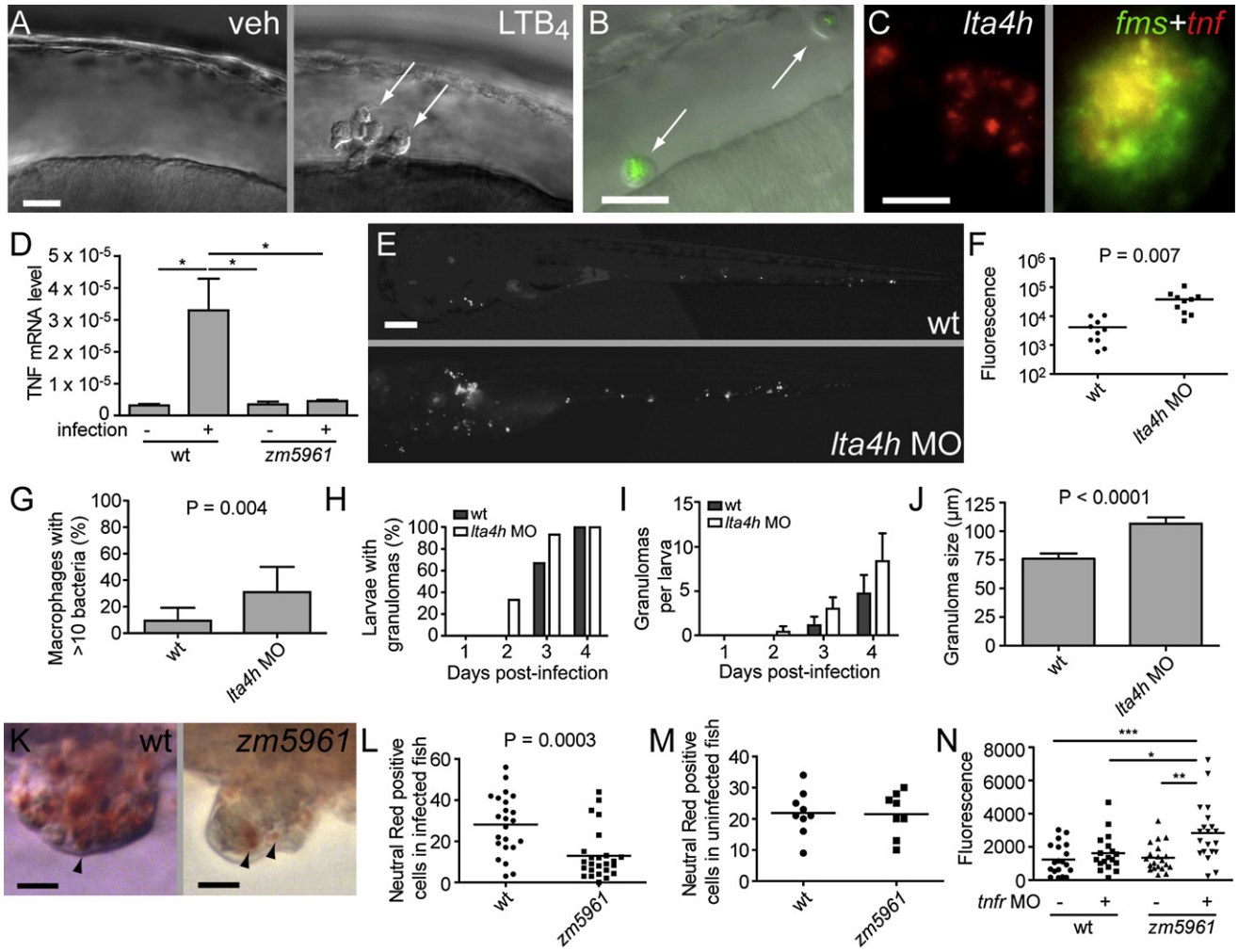

Figure 4. *lta4h* Deficiency Compromises TNF Induction and Phenotypically Resembles TNF Signaling Deficiency

(A) DIC image of HBV of 30 hpf-embryo 6 hr post-injection with vehicle (left) or 1.5 × 10^{-14} mol LTB_4 (right). Arrows, macrophages.

(B) Fluorescence and DIC overlay image of HBV of 30 hpf mutant *fh112* embryo (obtained from incross of *fh112*/+ heterozygotes) 6 hr post-injection with GFP-expressing Mm. Arrows, infected macrophages. After scoring for macrophage recruitment, genotype of embryos was identified based on cording phenotype at 4 dpi. The scale bar represents 20 μm.

(C) *lta4h* FISH showing staining of an early-stage granuloma 2 dpi (left); dual FISH showing *tnf* expression in macrophages of 4 dpi granuloma macrophages by demonstrating colocalization of the macrophage marker *fms* (green) and *tnf* (red). The scale bar represents 20 μm.

(D) Relative TNF mRNA levels (relative to a β-actin standard) assessed by qRT-PCR at 1 dpi following infection of 30 WT or *zm5961* larvae with 93 WT bacteria. Error bars represent the SEM. Representative of two independent experiments.

(E) Representative fluorescence images of control (top) or *lta4h* morphant (bottom) animals 3 dpi with 130 *erp* mutant bacteria. (n = 10 for each condition.) The scale bar represents 20 μm.

(F) Quantification of bacterial burdens by fluorescence pixel counts (FPC) of all animals from (D) at 6 dpi.

(G) Proportion of single macrophages containing > 10 bacteria in 15 control and 12 *lta4h* morphant animals at 3 dpi with 130 *erp* mutant bacteria. Error bars represent the SD.

(H–J) Serial assessment of granuloma formation in control (dark bars) and *lta4h* morphants (light bars) injected with 230 bacteria (n = 15 each) by fluorescence and DIC microscopy for 4 dpi.

(H) Percentage of animals with at least one granuloma over time. *lta4h* morphants form granulomas earlier; they are significantly more likely to have at least one granuloma than WT at 2 dpi ($p = 0.042$; Fisher's exact test).

(I) Average number of granulomas per fish over time. $p < 0.001$ when comparing both time post-infection and morphant status by two-way ANOVA. Error bars represent the SD.

(J) Morphometric analysis of control MO (WT) and *lta4h* MO granuloma size at 4 dpi; error bars represent the SEM.

(K) Neutral red labeling of granuloma macrophages in WT and *zm5961* granulomas. Arrowheads indicate examples of neutral red positive macrophages. Fish were infected with approximately 250 bacteria then neutral red stained at 4 dpi, six dpf. The scale bar represents 10 μm.

(L) Numbers of neutral red stained cells in the tails of infected WT and *zm5961* fish infected as described in (K). $p = 0.0003$ (Student's unpaired t test).

(M) Quantitation of neutral red stained cells in the tails of uninfected WT and *zm5961* fish at 6 dpf.

staining (Figures 4K–4M). Again similar to the TNF deficiency phenotype, the baseline apoptotic death in the granulomas was unchanged (Figure S3), suggesting that the necrotic death of granuloma macrophages was responsible for cording (Clay et al., 2008). Thus, *lta4h* morphants reproduced the TNF signaling deficiency phenotype.

To look for a genetic interaction between *lta4h* and the TNF pathway we asked whether a hypomorphic *lta4h* allele could serve as a genetic enhancer of altered TNF signaling. We produced TR1 or control morphants on either a WT or *zm5961* background. We infected all four groups with a low *Mm* inoculum that, at 4 dpi, did not yield increased bacterial burdens in either the TR1 deficient or *lta4h* deficient animals alone (Figure 4N). However, in combination, these two sub-phenotypic deficiencies resulted in increased bacterial burdens, suggesting a genetic interaction (Figure 4N). In sum, our data suggest that *lta4h* deficiencies interact genetically with the TNF signaling pathway, compromise TNF induction during infection and recapitulate the signature infection phenotypes of TNF signaling defects.

lta4h Deficiencies Result in an Immunoregulatory Phenotype

Having found that exogenous LTB_4 causes rapid induction of *tnf* mRNA, we asked if it could rescue the hypersusceptibility of *lta4h* deficiencies. We were surprised to find that it did not (Figures S4A and S4B). LTB_4 administration also failed to rescue the *tnf* mRNA induction defect in infected morphants (Figure 5A). These findings suggested that the hypersusceptibility observed in *lta4h* deficient animals occurs via induction of immunoregulatory pathways rather than directly by lack of LTB_4-induced proinflammatory functions. This immunoregulatory mechanism appears to be operant prior to infection, as LTB_4 failed to induce *tnf* expression even in uninfected morphants (Figure 5B).

The importance of anti-inflammatory eicosanoids is being recognized increasingly (Serhan, 2007) and we considered the possibility that they mediate the hypersusceptibility of *lta4h* deficient animals. Lipoxins are structurally related to the leukotrienes and can be synthesized via common intermediates and pathways (Figure 5C). Lipoxin A_4 (LXA_4) can be generated directly from an LTA_4 intermediate by either 12- or 15-lipoxygenase (12-LO; 15-LO) (Figure 5C), and both LXA_4 and LTB_4 are major eicosanoid products of adult fish macrophages (Pettitt et al., 1991; Serhan, 2007). We hypothesized that, in the absence of LTA4H, accumulating LTA_4 is redirected to LXA_4 production. Both LTB_4 and LXA_4 are induced during human and mouse TB (Bafica et al., 2005; el-Ahmady et al., 1997). 5-lipoxygenase (5-LO)-deficient mice lacking both LTB_4 and LXA_4 are resistant to *Mtb*, and administration of LXA_4 analogs restores susceptibility (Bafica et al., 2005). Moreover, in tissue culture assays virulent *Mtb* promotes necrosis of human macrophages via LXA_4 production (Chen et al., 2008; Divangahi et al., 2009). Finally, a chemical inhibitor of LTA4H increases lipoxin production in a mouse model of zymosan-induced peritonitis (Rao et al., 2007). Therefore, we sought to determine if *lta4h* mutant hypersusceptibility is due to the engagement of anti-inflammatory mechanisms accessed by increased lipoxin production.

Since mammalian studies suggest that lipoxins increase nitric oxide production, we compared inducible nitric oxide synthase (iNOS) expression in 4 dpi WT and *zm5961* fish by antibody staining (Clay et al., 2008; Paul-Clark et al., 2004). *zm5961* mutants had more iNOS-producing cells overall (2.2 fold over WT, $p = 0.008$) as well as within granulomas (2.3 fold over WT, $p = 0.01$) (Figures 5D and 5E), consistent with lipoxin excess in the mutants.

Next we took advantage of a well-characterized effect of lipoxins in mammals: the specific inhibition of neutrophil (and not macrophage) migration (Serhan, 2007). To determine if this lipoxin-mediated effect exists in the zebrafish, we injected LTB_4, a potent neutrophil chemoattractant, into the ear of WT larvae (Figure 1A), to which neutrophils migrate in response to *Escherichia coli* injection (Le Guyader et al., 2008). LTB_4 injection resulted in rapid neutrophil recruitment that was inhibited by the LTB_4 receptor blocker U75302 (Figures 5F and 5G and Figure S4C). U75302 did not produce hypersusceptibility to infection, adding to the evidence that susceptibility did not stem directly from LTB_4 deficiency (Figure S4D).

LTB_4-induced neutrophil migration was reduced by pre-administration of the lipoxin epimer 15-epi-LXA_4 into the caudal vein (Figures 5F and 5G). If the *lta4h* deficiency phenotype derives from a functional excess of lipoxins, then a similar effect should be apparent in *lta4h*-deficient fish. Both uninfected and infected morphants and mutants recruited fewer neutrophils than their WT counterparts (Figure 5H). Infection by virulent *Mtb* is itself reported to induce lipoxin production in cultured human macrophages (Chen et al., 2008). We too found reduced neutrophil recruitment upon infection of WT fish, consistent with infection-induced lipoxin production (Figure 5H). Yet, *lta4h* deficiencies produced a further reduction in neutrophil migration, suggesting substantial host-regulated lipoxin production. Reduction in LTB_4-induced neutrophil migration was also seen with chemical inhibition of LTA4H using bestatin (Figure S4E).

Since LXA_4 biosynthesis is dependent upon the activity of 12- or 15-lipoxygenases (Serhan, 2007) (Figure 5C), we asked if the neutrophil migration defect of the *lta4h* mutant was reversed by inhibiting these enzymes. Administration of 1 μM of the 15-lipoxygenase inhibitor PD146176 increased LTB_4-induced neutrophil migration to WT levels (Figure 5I). Notably, there appears to be a baseline lipoxin production in WT fish as PD146176 also increased their neutrophil recruitment to LTB_4 (Figure 5I). Finally, consistent with the specificity of lipoxins in reducing neutrophil and not macrophage migration (Serhan, 2007), we found no significant difference in LTB_4-induced macrophage migration to the HBV between WT and *zm5961* animals (Figure S4F). Thus, multiple lines of evidence pointed to a lipoxin excess in *lta4h*-deficient animals that was present at baseline and persisted during infection.

If *lta4h* deficiency compromises resistance to infection due to the observed lipoxin excess, then exogenous lipoxin should recreate the relevant infection phenotypes. A single intravenous

(N) Bacterial burdens (FPC) at 4 dpi with 75 bacteria in control or TR1 morphants in the background of either WT or *zm5961* animals. *$p < 0.05$; **$p < 0.01$; ***$p < 0.001$. (one-way ANOVA with Tukey's post-test; all other comparisons not significant).
See also Figure S2, Figure S3, and Movie S1.

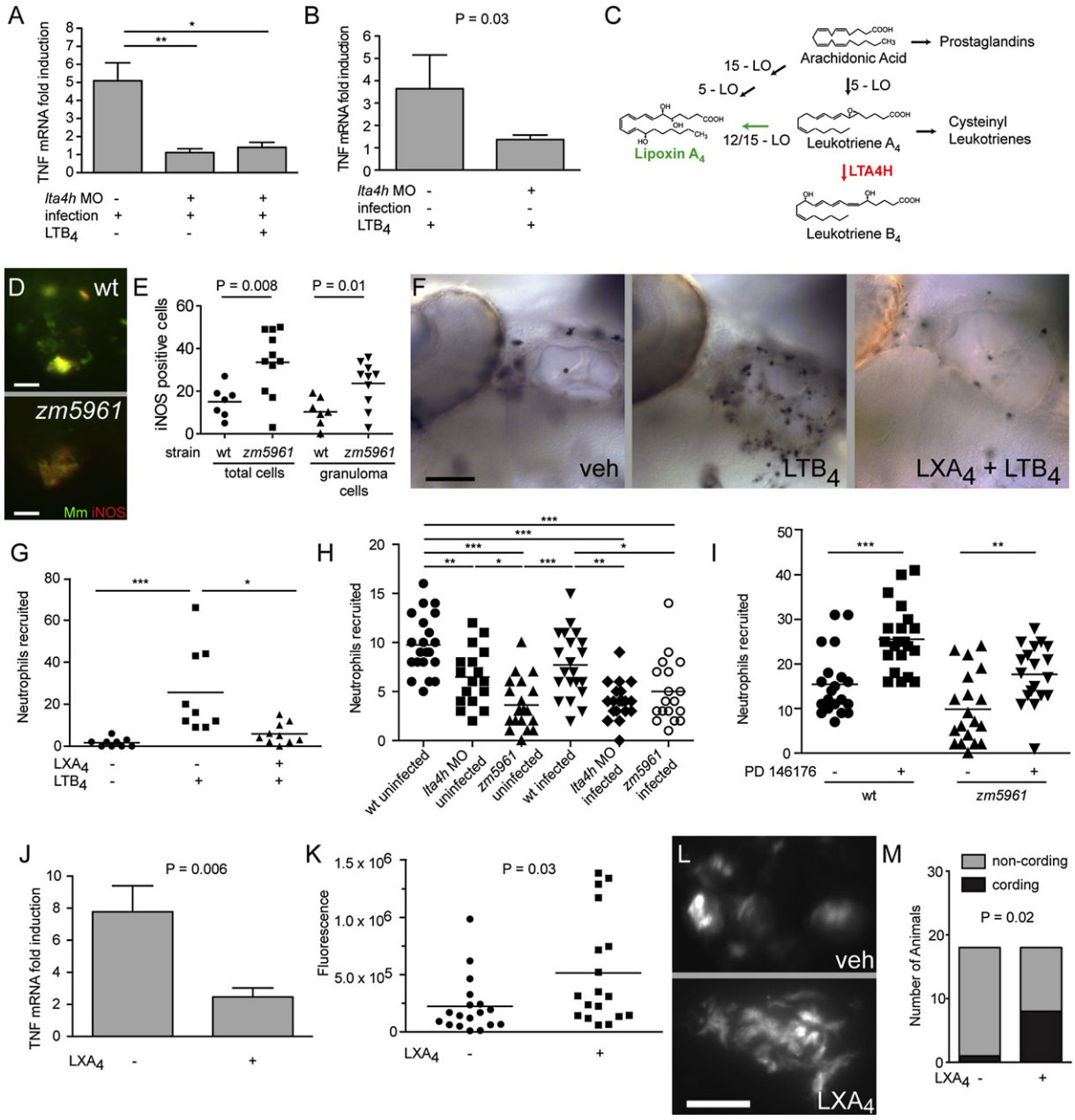

Figure 5. *lta4h* Deficiency Induces an Immunoregulatory Phenotype Recapitulated by Exogenous LXA_4

(A and B) *tnf* mRNA expression in control and *lta4h* morphant fish infected with Mm, injected with LTB_4, or both. Each bar represents a mean of three independent pools of 20–30 animals. Error bars represent the SD.

(A) *tnf* mRNA levels in control and morphant fish injected with 110 bacteria and at 1 dpi mock-injected or injected with 1.5×10^{-14} mol LTB_4 into the caudal vein 2.5 hr prior to RNA extraction. *$p < 0.05$; **$p < 0.01$ (one-way ANOVA. All other comparisons not significant).

(B) *tnf* mRNA levels in uninfected three dpf control or *lta4h* morphant animals 2.5 hr after injection of 1.5×10^{-14} mol LTB_4 into the caudal vein.

(C) Diagram of LTB_4 and LXA_4 biosynthetic pathways. Reduction of LTA4H activity (red) is hypothesized to result in increased synthesis of LXA_4 through pathway marked by green arrow.

(D) iNOS antibody staining in infected WT and *zm5961* animals. Green represents GFP-expressing Mm and red represents iNOS staining. Animals were infected with approximately 100-150 bacteria and fixed for antibody staining and imaging at 3 dpi. The scale bar represents 25 μm.

(E) Numbers of iNOS positive cells in WT and *zm5961* animals as described in (D) for both total number of iNOS positive cells in the tail ($p = 0.008$) and iNOS positive cells within granulomas ($p = 0.01$).

(F) Light microscopy images of Sudan black stained-neutrophils in right ear of three dpf animals injected with vehicle (left and middle) or 3.5×10^{-14} mol of LXA_4 (right) 10 hr prior and with vehicle (left) or 1.5×10^{-14} mol LTB_4 (middle and right) into the right ear 4 hr prior. The scale bar represents 50 μm.

(G) Mean number of neutrophils in ears of animals in (F). *$p < 0.05$; ***$p < 0.001$ (Kruskal-Wallis nonparametric one-way ANOVA with Dunn's post-test; other comparisons not significant).

dose of LXA_4 administered 3 days after infection resulted in a 3.2 fold decrease ($p = 0.006$) in *tnf* mRNA levels 8 hr later (Figure 5J). To determine if this lipoxin-induced TNF reduction was relevant for infection, we administered LXA_4 by caudal vein injection every 12 hr for 4 days starting 1 day after infection. LXA_4 treatment resulted in increased bacterial burden (Figure 5K) and cording frequency (Figures 5L and 5M).

In summary, despite the product of LTA4H being the strongly proinflammatory LTB_4, the predominant effect of *lta4h* deficiency during early mycobacterial infection likely results from increased lipoxins that dampen TNF-mediated protection. Additionally, the greater reduction in LTB_4-mediated neutrophil migration in the uninfected *zm5961* mutant than in the *lta4h* morphant in Figure 5H suggested a graduated relationship between LTA4H and TNF levels that would directly modulate susceptibility. To test this, we assessed *tnf* mRNA levels at 1 day postinfection in embryos injected with increasing doses of the *lta4h* MO. Increasing MO doses correlated inversely with *tnf* levels in the infected morphants suggesting that LTA4H activity levels may determine the extent of TNF induction at early time points (Figures S4G and S4H).

Heterozygosity at *LTA4H* and Susceptibility to Tuberculosis and Leprosy in Human Populations

Our data suggest that zebrafish LTA4H activity orchestrates the balance of pro- and anti-inflammatory eicosanoids so as to affect innate immune resistance to mycobacterial infection. We hypothesized that polymorphisms affecting levels of leukotriene and lipoxin production in humans might influence susceptibility to mycobacterial diseases. Single nucleotide polymorphisms (SNPs) at the human *LTA4H* locus (Figures 6A and 6B) define a haplotype associated with significant differences in LTB_4 levels following ionomycin stimulation of granulocytes of healthy individuals (Helgadottir et al., 2006). We examined whether these *LTA4H* polymorphisms were associated with susceptibility to TB and to another major mycobacterial disease, leprosy.

Vietnamese patients with pulmonary or meningeal TB were compared to Vietnamese controls. All patients and controls were of Kinh ethnicity (Hawn et al., 2006 and Supplemental Information). We genotyped six *LTA4H* SNPs in 692 cases and 759 controls from this cohort (Table 1). At all six SNPs, genotypes conformed to Hardy Weinberg Equilibrium (HWE) in the control series, but deviated significantly from HWE in the case series. At each site among the cases, fewer heterozygotes were present than expected by HWE expectation, suggesting that heterozygosity at this locus might be protective against TB.

Comparison of frequencies of heterozygotes versus homozygotes among TB cases and controls yielded odds ratios (ORs) < 1.0 at all six SNPs (Table 1). Adjusting for multiple comparisons, association of heterozygosity and lower incidence of TB were significant at rs1978331 and rs2660898, the two SNPs intragenic in *LTA4H* with common minor allele frequencies. The heterozygous effect remained after adjusting for gender and stratifying for age at diagnosis (Table S1). A strong association of heterozygosity with lower incidence of TB was also noted for 2-SNP haplotypes constructed from rs1978331 and rs2660898 (OR = 0.65, $p = 0.0003$, Table S2). Heterozygosity at *LTA4H* was associated with protection from both pulmonary and meningeal TB (Table S2), consistent with the early involvement of the pathway in mycobacterial pathogenesis revealed in the zebrafish (Figure 3B).

Meningeal TB carries a high mortality (Thwaites et al., 2000): 27 of 209 patients or 13% in this cohort. We tested whether heterozygosity at *LTA4H* was associated with mortality among the patients with meningeal TB (Figure 6C). Among meningeal TB patients heterozygous at both intragenic SNPs at *LTA4H*, mortality was 4%, whereas among meningeal TB patients not heterozygous at these two sites, mortality was 16% ($p = 0.025$).

In order to test whether heterozygosity at *LTA4H* protected against another mycobacterial disease in a different population in a different environment, we evaluated a cohort of persons from Nepal, all of whom were exposed to leprosy (Misch et al., 2008). The ability of host macrophages to control mycobacterial growth is an important determinant of whether an individual exposed to *M. leprae* develops low burden (paucibacillary) versus high burden (multibacillary) leprosy (Scollard et al., 2006). Furthermore, TNF appears to protect exposed persons from developing multibacillary leprosy yet is implicated in development of hypersensitivity (erythema nodosum leprosum, or ENL) in a subset of patients with multibacillary disease (Scollard et al., 2006). Given the central role of TNF signaling in the *lta4h*-associated phenotype of the zebrafish, we evaluated the leprosy patients in three groups, defined by paucibacillary leprosy (the baseline exposed group), multibacillary leprosy without ENL, and multibacillary leprosy with ENL.

To evaluate associations of heterozygosity at *LTA4H* with leprosy, we genotyped only rs1978331 and rs2660898, the two SNPs for which heterozygosity was associated with protection from TB with significant P values after correction for multiple tests.

(H) Mean number of neutrophils in ears of three dpf controls, *lta4h* morphant and *zm5961* mutant animals either infected (135 CFU) or mock-infected 1 day prior then injected into right ear with 1.5×10^{-14} mol LTB_4 and scored 4 hr later. *$p < 0.05$; **$p < 0.01$; ***$p < 0.001$ (One-way ANOVA with Tukey's post-test; all other pairwise comparisons not significant).

(I) Mean number of neutrophils recruited to ears of three dpf uninfected animals injected into right ear with 1.5×10^{-14} mol LTB_4 after overnight exposure to vehicle or 1 μM PD146176. **$p < 0.01$; ***$p < 0.001$ (One-way ANOVA with Tukey's post-test).

(J) Mean *tnf* levels relative to uninfected controls in animals (25–30 per group) 8 hr after single dose of 3.5×10^{-14} mol LXA_4 or vehicle injected into caudal vein 3 dpi with either mock-infection or with 158 bacteria. Error bars, SD. Representative of three independent experiments.

(K) Mean bacterial burdens (FPC) in 5 dpi WT fish infected at two dpf with 212 CFU and, beginning 1 dpi, given injections of 3.5×10^{-14} mol of LXA_4 or vehicle every 12 hr into the caudal vein for 4 days (n = 18 per group). $p = 0.0283$ (Unpaired t test with Welch's correction to account for unequal variances).

(L) Examples from (K) of non-cording bacteria within granuloma in vehicle-injected fish and cording bacteria in LXA_4-injected fish at 5 dpi. The scale bar represents 30 μm.

(M) Quantitation of cording from (K and L) at 5 dpi. $p = 0.018$ by Fisher's exact test of a contingency table.

See also Figure S4.

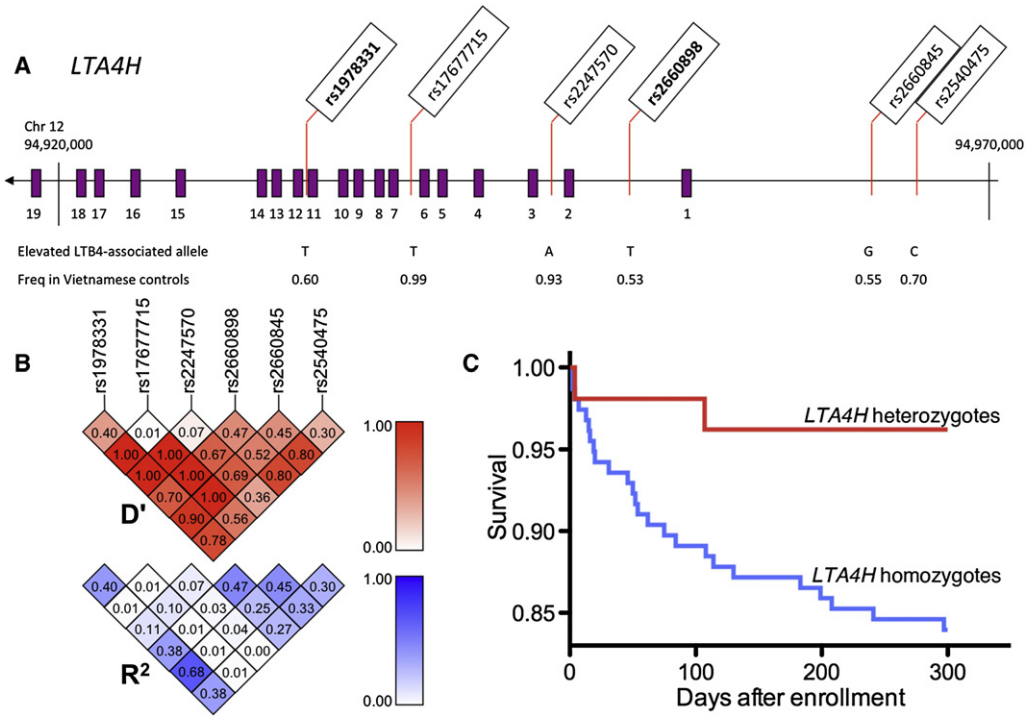

Figure 6. *LTA4H* and Susceptibility to Human Mycobacterial Diseases

(A) *LTA4H* exons are shown as purple rectangles. Below the *LTA4H* gene are indicated the allele at each SNP associated with higher levels of LTB_4 after ionomycin stimulation of granulocytes (Helgadottir et al., 2006) and the frequencies of these alleles among Vietnamese controls. SNPs rs1978331 and rs2660898, for which significant associations were found in this study, are in bold type.

(B) Linkage disequilibrium between SNPs, based on D-prime (D′) and R-squared (R^2) values, were calculated for Vietnamese controls and are shown as triangles. The minor allele frequency is shown adjacent to each corresponding SNP.

(C) Mortality from meningeal TB for patients heterozygous for both *LTA4H* SNPs rs1978331 and rs2660898 (n = 53, red curve) and for patients homozygous at one or both SNPs (n = 156, blue curve). Difference between the curves is significant at p = 0.025.

Among the leprosy patients, genotypes at each SNP conformed to Hardy Weinberg Equilibrium for persons with paucibacillary leprosy or with multibacillary leprosy with ENL, but not for persons with multibacillary leprosy without ENL, among whom there were fewer heterozygotes than expected (Table 1). Odds ratios for association of heterozygosity with protection from multibacillary leprosy without ENL were < 1.0 and significant for both SNPs. The association of heterozygosity with lower incidence of multibacillary leprosy without ENL was retained for 2-SNP haplotypes constructed from rs1978331 and rs2660898 (OR = 0.68, p = 0.016, Table S2). Heterozygosity at *LTA4H* was not associated with multibacillary leprosy with ENL response. In this subset of patients, exposures to other infections and/or genetic factors other than *LTA4H* may lead to elevated levels of TNF and other cytokines, so as both to abrogate the protective effect of heterozygosity at *LTA4H* and to stimulate hypersensitivity.

Findings from the TB and leprosy studies together suggest association of heterozygosity for functionally different haplotypes at *LTA4H* with human mycobacterial disease. For tuberculosis, heterozygosity at *LTA4H* was associated with protection from infection and with lower mortality among patients with severe disease. For leprosy, heterozygosity at *LTA4H* confers protection from development of severe disease among exposed persons.

DISCUSSION

The zebrafish/Mm infection model has enabled detailed analysis of the key milestones of mycobacterial infection affected by genetic perturbations in a live, transparent organism. The emergent mutant classes from our screen expand our understanding of pathogenesis during the innate immune response to infection and confirm predictions from human epidemiological studies on humans following exposures to Mtb (Cobat et al., 2009).The granuloma-defective mutants reinforce our recent findings with the bacterial RD1 and host MMP9 mutants that early granuloma formation favors bacterial expansion rather than restricting infection (Davis and Ramakrishnan, 2009; Volkman et al., 2010). Mapping of their affected loci may lead to other host determinants that enhance granuloma formation. Similarly, the class of resistant mutants with more restricted bacterial growth may lead to immunoregulators that limit mycobacterial clearance.

Unexpectedly, our analysis of the hypersusceptible *lta4h* mutant has also uncovered an immunoregulatory pathway, in this case increased immunoregulation likely via a functional excess of the anti-inflammatory lipoxins. While virulent mycobacteria can induce lipoxins (Chen et al., 2008), this mycobacterially-induced lipoxin production is not saturating. LTA4H deficiency can increase anti-inflammatory activity further to the dramatic

Table 1. Associations of Tuberculosis and Leprosy with Heterozygosity at *LTA4H*

SNP	Group	N	Genotype Frequency 00[a]	01[a]	11[a]	HWE[b] p value	Heterozygosity Model OR[c]	p value	p adj[d]
Tuberculosis in Vietnam									
rs1978331 T/C	TB	657	0.406	0.397	0.196	<0.0001	0.71	0.002	0.011
	Controls	748	0.350	0.480	0.170	0.83			
rs17677715 T/C	TB	640	0.988	0.009	0.003	<0.0001	0.69	0.476	ns
	Controls	741	0.987	0.013	0.000	0.85			
rs2247570 A/G	TB	658	0.891	0.093	0.017	<0.0001	0.66	0.017	ns
	Controls	743	0.860	0.133	0.007	0.59			
rs2660898 T/G	TB	658	0.353	0.400	0.248	<0.0001	0.64	0.00004	0.0003
	Controls	751	0.277	0.509	0.214	0.56			
rs2660845 G/A	TB	645	0.310	0.428	0.262	0.0003	0.84	0.099	ns
	Controls	724	0.314	0.472	0.214	0.22			
rs2540475 C/T	TB	660	0.529	0.364	0.108	0.003	0.82	0.068	ns
	Controls	739	0.497	0.411	0.092	0.66			
Leprosy in Nepal									
rs1978331 T/C	MB w/o ENL*	436	0.336	0.435	0.229	0.01	0.62	0.001	
	MB w/ ENL*	120	0.258	0.492	0.250	0.81	0.78	0.24	
	PB*	328	0.274	0.555	0.171	0.05			
rs2660898 T/G	MB w/o ENL*	386	0.509	0.372	0.120	0.01	0.70	0.021	
	MB w/ ENL*	113	0.372	0.504	0.124	0.42	1.21	0.38	
	PB*	315	0.466	0.457	0.078	0.18			

* Multibacillary leprosy, MB, without or with erythema nodosum leprosum, ENL; paucibacillary leprosy, PB. See also Table S1 and Table S2.
[a] For each SNP, 0 represents the allele associated with higher levels of LTB_4 (Figure 6A).
[b] P values for deviations from Hardy Weinberg Equilibrium (HWE).
[c] For each SNP, odds ratios (OR) calculated for heterozygosity (01) versus homozygosity (00+11) for cases versus controls.
[d] p values adjusted by Bonferroni correction for multiple tests.

detriment of the host. Indeed we find that the anti-inflammatory state of *lta4h* mutants precedes mycobacterial infection; baseline lipoxin excess in the uninfected state limits TNF production from early in infection. Host interactions with commensal flora may trigger this baseline lipoxin excess in *lta4h* deficient hosts making them unable to mount a fully effective proinflammatory response early after mycobacterial exposure.

This work suggests that LTA4H activity, while required for LTB_4 proinflammatory functions in a variety of circumstances, serves to determine levels of key anti-inflammatory molecules in early TB. Thus LTA4H may operate as a genetically encoded rheostat within an eicosanoid circuit, influencing the relative amount of LXA_4 produced from LTA_4 (Figure 7).

Our analyses of mycobacterial diseases in human populations extend this model. We observe significant associations of heterozygosity at the *LTA4H* locus with protection from TB in a Vietnamese cohort, and with protection from multibacillary leprosy in a Nepali cohort. Heterozygosity for haplotypes associated with lower versus higher production of LTB_4 may reflect an optimal balance of pro- and anti-inflammatory eicosanoids during mycobacterial infection. *LTA4H* genotypes associated with lower LTB_4 production may be deficient in TNF-mediated protection from mycobacterial infection, as in the zebrafish, resulting in clinical TB or more severe leprosy. At the same time, *LTA4H* genotypes that maximize proinflammatory responses may experience increased susceptibility through increased immunopathology (Figure 7).

Mycobacterial infection itself induces LTB_4 (Bafica et al., 2005; el-Ahmady et al., 1997) and is recognized to mediate virulence via induction of host immunopathology (Kaushal et al., 2002; Steyn et al., 2002). In BCG-infected TNF-deficient mice, an optimal TNF replacement dose decreases bacterial burdens and increases mouse survival; greater doses of TNF decrease bacterial burden yet diminish host survival by induction of immunopathology (Bekker et al., 2000). Moreover, a recent study implicates a mycobacterial adenylate cyclase in promoting virulence and immunopathology through increased TNF levels (Agarwal et al., 2009).

Immunosuppressive agents have long been used as adjuvant treatment for certain forms of TB and TB recalcitrant to therapies. These include corticosteroids, TNF blocking agents, and most recently agents intercepting certain leukotriene pathways (Blackmore et al., 2008; Hardwick et al., 2006; Thwaites et al., 2004). Another immediate clinical implication of these findings is that among patients with TB meningitis, *LTA4H* genotypes

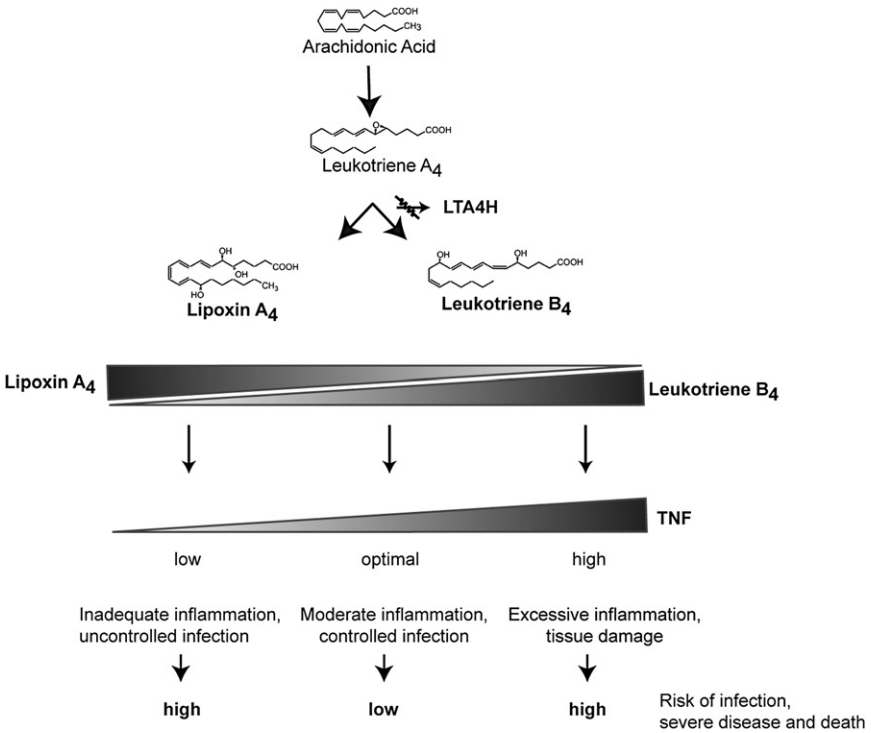

Figure 7. Model of *lta4h* Effects on Eicosanoid Balance

Variations in LTA4H levels or activity, represented by the rheostat symbol, influence the balance between proinflammatory LTB_4 and anti-inflammatory LXA_4. High levels of LXA_4 inhibit TNF production, resulting in exuberant intracellular bacterial growth, increased granuloma formation, increased macrophage death and the cording morphology typical of extracellular mycobacteria. Although WT levels of TNF are protective during infection, excessive levels of TNF may produce increased immunopathology, resulting in worse outcome from mycobacterial infections.

may influence outcome. Our findings underscore the potential for pharmacological agents that modulate lipoxins and other immunoregulators to obtain maximal control of mycobacterial infection.

EXPERIMENTAL PROCEDURES

Zebrafish and Bacterial Strains

Wild-type AB zebrafish larvae were maintained and infected by microinjection into the caudal vein or HBV as described (Cosma et al., 2006). Mm strain M (ATCC #BAA-535) and mutants derived from it that were rendered red or green fluorescent were used (Clay et al., 2008; Cosma et al., 2006). Bacterial counts were determined by plating (Clay et al., 2008) or by quantitating fluorescence pixel counts in live animals as detailed in Extended Experimental Procedures.

Zebrafish Mutagenesis, Screening, and Positional Cloning

Early pressure gynogenetic diploids were generated (Johnson et al., 1995) and infected by caudal vein injection at 48 hr post-fertilization (hpf) with 150–200 green fluorescent bacteria. Putative mutants were outcrossed to the WT WIK strain and mutants and carriers identified by random crosses between siblings. Bulk segregant analysis was performed on mutant progeny and phenotypically WT animals collected from incrosses (Bahary et al., 2004). The retroviral insertion mutant *zm5961* was identified from a sperm library maintained by Znomics (Portland, OR, USA).

lta4h MOs

MOs were obtained from Genetools (Eugene, OR, USA) and injected at the one- to four-cell stage as described (Clay et al., 2008).

In Situ Hybridization and Antibody Staining

Fluorescent in situ hybridization was performed as described (Clay et al., 2007, 2008) and detailed in Extended Experimental Procedures. Antibody staining for MPO and iNOS was performed as described (Clay et al., 2007, 2008). For Annexin V staining, a 1/10 dilution of Annexin V-AlexaFluor 488 (Invitrogen) was microinjected into the caudal vein of 4 dpi animals and quantitation was performed 4 hr later.

Neutral Red and Sudan Black Staining

Neutral red and Sudan black staining was performed as described (Herbomel et al., 2001; Le Guyader et al., 2008).

Leukotriene B_4 and Lipoxin Injections

Leukotriene B_4 (Cayman Chemical), Lipoxin A_4 (Calbiochem) or 15-epi Lipoxin A_4 (Calbiochem) was microinjected at the concentrations indicated into the hindbrain, caudal vein or right ear as described (Cosma et al., 2006; Le Guyader et al., 2008) and detailed in Extended Experimental Procedures (Cosma et al., 2006; Le Guyader et al., 2008).

Eicosanoid Pathway Inhibitors

Bestatin (Cayman Chemical), U75302 (BIOMOL) or PD-146176 (BIOMOL) were administered by soaking starting at 2 dpf.

Clinical Studies

The case-control study of TB in Vietnam (Hawn et al., 2006) and the case-case comparison study of leprosy in Nepal (Misch et al., 2008) have been previously described.

All protocols were carried out in accordance with human subjects review committees at each site, the Oxford Tropical Research Ethics Committee, the Nepal Health Research Council, the University of Washington (Seattle, WA, USA), the University of Medicine and Dentistry of New Jersey (Newark, NJ, USA), and the Western Institutional Review Board (Olympia, WA, USA).

Six SNPs within the *LTA4H* gene, previously described as part of the HapK haplotype (Helgadottir et al., 2006), were genotyped using MassARRAY (Sequenom), as described (Hawn et al., 2006). Statistical analyses are detailed in Extended Experimental Procedures.

SUPPLEMENTAL INFORMATION

Supplemental Information includes Extended Experimental Procedures, four figures, two tables, and one movie and can be found with this article online at doi:10.1016/j.cell.2010.02.013.

ACKNOWLEDGMENTS

We thank D. Payan for suggesting the zebrafish; J. Bennett and C.B. Wilson for encouragement and help in obtaining zebrafish facilities; C.N. Serhan for advice on eicosanoids; K. Winglee for developing FPC analysis; A. Carmany-Rampey, P. Grant, and C. Miller for setting up early pressure screens; R. Kim and D. Beery for assistance with microinjections; J. Cameron and L. Swaim for fish husbandry; H. Clay for the *tnf/fms* image; and A. Huttenlocher

for the *mpo* antibody. For the human studies, we gratefully acknowledge all participants and the clinical staff of the Hospital of Tropical Diseases (particularly T.T.H. Chau and G. Thwaites), Pham Ngoc Thach Hospital for Tuberculosis and Lung Disease (particularly N.H. Dung, N.T.B. Yen and N.T.N. Lan), and Hung Vuong Obstetric Hospital (N.T. Hieu) for facilitating the patient sample collection, M. Janer and S. Li for DNA genotyping, and M.K. Lee for statistical advice. This work was supported by the Burroughs Wellcome Fund (L.R. and T.R.H.), the Akibene Foundation and the Keck Foundation (L.R.), the National Institutes of Health (L.R. and M.C.K.), an American Cancer Society Postdoctoral Fellowship and National Institutes of Health Bacterial Pathogenesis Training Grant (D.M.T.), the Odland Endowment of the University of Washington, Dermatology Foundation Dermatologist Investigator Research Fellowship, National Institutes of Health National Research Service Award, and the American Skin Association (J.C.V.), the Human Frontiers Science Program (G.S.W.), the Dana Foundation (T.R.H. and S.J.D.), the Heiser Program for Research in Tuberculosis and Leprosy (T.R.H.), the Wellcome Trust of Great Britain (S.J.D.) and the Leprosy Mission International (D.A.H.). C.B.M. is an investigator with the Howard Hughes Medical Institute. M.C.K. is an American Cancer Society Professor.

Received: April 15, 2009
Revised: July 10, 2009
Accepted: February 10, 2010
Published: March 4, 2010

REFERENCES

Agarwal, N., Lamichhane, G., Gupta, R., Nolan, S., and Bishai, W.R. (2009). Cyclic AMP intoxication of macrophages by a Mycobacterium tuberculosis adenylate cyclase. Nature *460*, 98–102.

Alter, A., Alcais, A., Abel, L., and Schurr, E. (2008). Leprosy as a genetic model for susceptibility to common infectious diseases. Hum. Genet. *123*, 227–235.

Bafica, A., Scanga, C.A., Serhan, C., Machado, F., White, S., Sher, A., and Aliberti, J. (2005). Host control of Mycobacterium tuberculosis is regulated by 5-lipoxygenase-dependent lipoxin production. J. Clin. Invest. *115*, 1601–1606.

Bahary, N., Davidson, A., Ransom, D., Shepard, J., Stern, H., Trede, N., Zhou, Y., Barut, B., and Zon, L.I. (2004). The Zon laboratory guide to positional cloning in zebrafish. Methods Cell Biol. *77*, 305–329.

Beattie, C.E., Raible, D.W., Henion, P.D., and Eisen, J.S. (1999). Early pressure screens. Methods Cell Biol. *60*, 71–86.

Bekker, L.G., Moreira, A.L., Bergtold, A., Freeman, S., Ryffel, B., and Kaplan, G. (2000). Immunopathologic effects of tumor necrosis factor alpha in murine mycobacterial infection are dose dependent. Infect. Immun. *68*, 6954–6961.

Blackmore, T.K., Manning, L., Taylor, W.J., and Wallis, R.S. (2008). Therapeutic use of infliximab in tuberculosis to control severe paradoxical reaction of the brain and lymph nodes. Clin. Infect. Dis. *47*, e83–e85.

Chen, M., Divangahi, M., Gan, H., Shin, D.S., Hong, S., Lee, D.M., Serhan, C.N., Behar, S.M., and Remold, H.G. (2008). Lipid mediators in innate immunity against tuberculosis: opposing roles of PGE2 and LXA4 in the induction of macrophage death. J. Exp. Med. *205*, 2791–2801.

Clay, H., Davis, J., Beery, D., Huttenlocher, A., Lyons, S., and Ramakrishnan, L. (2007). Dichotomous Role of the Macrophage in Early Mycobacterium marinum Infection of the Zebrafish. Cell Host Microbe *2*, 29–39.

Clay, H., Volkman, H.E., and Ramakrishnan, L. (2008). Tumor necrosis factor signaling mediates resistance to mycobacteria by inhibiting bacterial growth and macrophage death. Immunity *29*, 283–294.

Cobat, A., Gallant, C.J., Simkin, L., Black, G.F., Stanley, K., Hughes, J., Doherty, T.M., Hanekom, W.A., Eley, B., Jais, J.P., et al. (2009). Two loci control tuberculin skin test reactivity in an area hyperendemic for tuberculosis. J. Exp. Med. *206*, 2583–2591.

Cosma, C.L., Davis, J.M., Swaim, L.E., Volkman, H., and Ramakrishnan, L. (2006). Zebrafish and Frog Models of Mycobacterium marinum Infection. In Current Protocols in Microbiology (New York: John Wiley and sons, Inc).

Davis, J.M., Clay, H., Lewis, J.L., Ghori, N., Herbomel, P., and Ramakrishnan, L. (2002). Real-time visualization of mycobacterium-macrophage interactions leading to initiation of granuloma formation in zebrafish embryos. Immunity *17*, 693–702.

Davis, J.M., and Ramakrishnan, L. (2009). The role of the granuloma in expansion and dissemination of early tuberculous infection. Cell *136*, 37–49.

Divangahi, M., Chen, M., Gan, H., Desjardins, D., Hickman, T.T., Lee, D.M., Fortune, S., Behar, S.M., and Remold, H.G. (2009). Mycobacterium tuberculosis evades macrophage defenses by inhibiting plasma membrane repair. Nat. Immunol. *10*, 899–906.

el-Ahmady, O., Mansour, M., Zoeir, H., and Mansour, O. (1997). Elevated concentrations of interleukins and leukotriene in response to Mycobacterium tuberculosis infection. Ann. Clin. Biochem. *34*, 160–164.

Flynn, J.L., Goldstein, M.M., Chan, J., Triebold, K.J., Pfeffer, K., Lowenstein, C.J., Schreiber, R., Mak, T.W., and Bloom, B.R. (1995). Tumor necrosis factor-alpha is required in the protective immune response against Mycobacterium tuberculosis in mice. Immunity *2*, 561–572.

Fortin, A., Abel, L., Casanova, J.L., and Gros, P. (2007). Host genetics of mycobacterial diseases in mice and men: forward genetic studies of BCG-osis and tuberculosis. Annu. Rev. Genomics Hum. Genet. *8*, 163–192.

Goldman, G., Welbourn, R., Kobzik, L., Valeri, C.R., Shepro, D., and Hechtman, H.B. (1993). Lavage with leukotriene B4 induces lung generation of tumor necrosis factor-alpha that in turn mediates neutrophil diapedesis. Surgery *113*, 297–303.

Haeggstrom, J.Z. (2004). Leukotriene A4 hydrolase/aminopeptidase, the gatekeeper of chemotactic leukotriene B4 biosynthesis. J. Biol. Chem. *279*, 50639–50642.

Hardwick, C., White, D., Morris, E., Monteiro, E.F., Breen, R.A., and Lipman, M. (2006). Montelukast in the treatment of HIV associated immune reconstitution disease. Sex. Transm. Infect. *82*, 513–514.

Hawn, T.R., Dunstan, S.J., Thwaites, G.E., Simmons, C.P., Thuong, N.T., Lan, N.T., Quy, H.T., Chau, T.T., Hieu, N.T., Rodrigues, S., et al. (2006). A polymorphism in Toll-interleukin 1 receptor domain containing adaptor protein is associated with susceptibility to meningeal tuberculosis. J. Infect. Dis. *194*, 1127–1134.

Helgadottir, A., Manolescu, A., Helgason, A., Thorleifsson, G., Thorsteinsdottir, U., Gudbjartsson, D.F., Gretarsdottir, S., Magnusson, K.P., Gudmundsson, G., Hicks, A., et al. (2006). A variant of the gene encoding leukotriene A4 hydrolase confers ethnicity-specific risk of myocardial infarction. Nat. Genet. *38*, 68–74.

Herbomel, P., Thisse, B., and Thisse, C. (2001). Zebrafish early macrophages colonize cephalic mesenchyme and developing brain, retina, and epidermis through a M-CSF receptor-dependent invasive process. Dev. Biol. *238*, 274–288.

Johnson, S.L., Africa, D., Horne, S., and Postlethwait, J.H. (1995). Half-tetrad analysis in zebrafish: mapping the ros mutation and the centromere of linkage group I. Genetics *139*, 1727–1735.

Kaushal, D., Schroeder, B.G., Tyagi, S., Yoshimatsu, T., Scott, C., Ko, C., Carpenter, L., Mehrotra, J., Manabe, Y.C., Fleischmann, R.D., et al. (2002). Reduced immunopathology and mortality despite tissue persistence in a Mycobacterium tuberculosis mutant lacking alternative sigma factor, SigH. Proc. Natl. Acad. Sci. USA *99*, 8330–8335.

Keane, J., Gershon, S., Wise, R.P., Mirabile-Levens, E., Kasznica, J., Schwieterman, W.D., Siegel, J.N., and Braun, M.M. (2001). Tuberculosis associated with infliximab, a tumor necrosis factor alpha-neutralizing agent. N. Engl. J. Med. *345*, 1098–1104.

Koch, R. (1882). The Aetiology of Tuberculosis (New York: National Tuberculosis Association).

Le Guyader, D., Redd, M.J., Colucci-Guyon, E., Murayama, E., Kissa, K., Briolat, V., Mordelet, E., Zapata, A., Shinomiya, H., and Herbomel, P. (2008). Origins and unconventional behavior of neutrophils in developing zebrafish. Blood *111*, 132–141.

Liew, F.Y., Xu, D., Brint, E.K., and O'Neill, L.A. (2005). Negative regulation of toll-like receptor-mediated immune responses. Nat. Rev. Immunol. *5*, 446–458.

Middlebrook, G., Dobos, R.J., and Pierce, C. (1947). Virulence and morphological characteristics of mammalian tubercle bacilli. J. Exp. Med. *86*, 175–184.

Misch, E.A., Macdonald, M., Ranjit, C., Sapkota, B.R., Wells, R.D., Siddiqui, M.R., Kaplan, G., and Hawn, T.R. (2008). Human TLR1 Deficiency Is Associated with Impaired Mycobacterial Signaling and Protection from Leprosy Reversal Reaction. PLoS Negl. Trop. Dis. *2*, e231.

Murayama, E., Kissa, K., Zapata, A., Mordelet, E., Briolat, V., Lin, H.F., Handin, R.I., and Herbomel, P. (2006). Tracing hematopoietic precursor migration to successive hematopoietic organs during zebrafish development. Immunity *25*, 963–975.

Nasevicius, A., and Ekker, S.C. (2000). Effective targeted gene 'knockdown' in zebrafish. Nat. Genet. *26*, 216–220.

Orning, L., Krivi, G., and Fitzpatrick, F.A. (1991). Leukotriene A4 hydrolase. Inhibition by bestatin and intrinsic aminopeptidase activity establish its functional resemblance to metallohydrolase enzymes. J. Biol. Chem. *266*, 1375–1378.

Pan, H., Yan, B.S., Rojas, M., Shebzukhov, Y.V., Zhou, H., Kobzik, L., Higgins, D.E., Daly, M.J., Bloom, B.R., and Kramnik, I. (2005). Ipr1 gene mediates innate immunity to tuberculosis. Nature *434*, 767–772.

Paul-Clark, M.J., Van Cao, T., Moradi-Bidhendi, N., Cooper, D., and Gilroy, D.W. (2004). 15-epi-lipoxin A4-mediated induction of nitric oxide explains how aspirin inhibits acute inflammation. J. Exp. Med. *200*, 69–78.

Peters-Golden, M., and Henderson, W.R., Jr. (2007). Leukotrienes. N. Engl. J. Med. *357*, 1841–1854.

Pettitt, T.R., Rowley, A.F., Barrow, S.E., Mallet, A.I., and Secombes, C.J. (1991). Synthesis of lipoxins and other lipoxygenase products by macrophages from the rainbow trout, Oncorhynchus mykiss. J. Biol. Chem. *266*, 8720–8726.

Rao, N.L., Dunford, P.J., Xue, X., Jiang, X., Lundeen, K.A., Coles, F., Riley, J.P., Williams, K.N., Grice, C.A., Edwards, J.P., et al. (2007). Anti-inflammatory activity of a potent, selective leukotriene A4 hydrolase inhibitor in comparison with the 5-lipoxygenase inhibitor zileuton. J. Pharmacol. Exp. Ther. *321*, 1154–1160.

Russell, D.G. (2007). Who puts the tubercle in tuberculosis? Nat. Rev. Microbiol. *5*, 39–47.

Scollard, D.M., Adams, L.B., Gillis, T.P., Krahenbuhl, J.L., Truman, R.W., and Williams, D.L. (2006). The continuing challenges of leprosy. Clin. Microbiol. Rev. *19*, 338–381.

Serhan, C.N. (2007). Resolution phase of inflammation: novel endogenous anti-inflammatory and proresolving lipid mediators and pathways. Annu. Rev. Immunol. *25*, 101–137.

Steyn, A.J., Collins, D.M., Hondalus, M.K., Jacobs, W.R., Jr., Kawakami, R.P., and Bloom, B.R. (2002). Mycobacterium tuberculosis WhiB3 interacts with RpoV to affect host survival but is dispensable for in vivo growth. Proc. Natl. Acad. Sci. USA *99*, 3147–3152.

Swaim, L.E., Connolly, L.E., Volkman, H.E., Humbert, O., Born, D.E., and Ramakrishnan, L. (2006). Mycobacterium marinum infection of adult zebrafish causes caseating granulomatous tuberculosis and is moderated by adaptive immunity. Infect. Immun. *74*, 6108–6117.

Thwaites, G., Chau, T.T., Mai, N.T., Drobniewski, F., McAdam, K., and Farrar, J. (2000). Tuberculous meningitis. J. Neurol. Neurosurg. Psychiatry *68*, 289–299.

Thwaites, G.E., Nguyen, D.B., Nguyen, H.D., Hoang, T.Q., Do, T.T., Nguyen, T.C., Nguyen, Q.H., Nguyen, T.T., Nguyen, N.H., Nguyen, T.N., et al. (2004). Dexamethasone for the treatment of tuberculous meningitis in adolescents and adults. N. Engl. J. Med. *351*, 1741–1751.

Tobin, D.M., and Ramakrishnan, L. (2008). Comparative pathogenesis of Mycobacterium marinum and Mycobacterium tuberculosis. Cell. Microbiol. *10*, 1027–1039.

Volkman, H.E., Pozos, T.C., Zheng, J., Davis, J.M., Rawls, J.F., and Ramakrishnan, L. (2010). Tuberculous granuloma induction via interaction of a bacterial secreted protein with host epithelium. Science *327*, 466–469.

Wolf, A.J., Linas, B., Trevejo-Nunez, G.J., Kincaid, E., Tamura, T., Takatsu, K., and Ernst, J.D. (2007). Mycobacterium tuberculosis infects dendritic cells with high frequency and impairs their function in vivo. J. Immunol. *179*, 2509–2519.